電壓多根解의 特性 및 誘導電動機負荷를 갖는 系統에 있어서의 電壓安定性

論 文
34~1~3

Properties of Multiple Load Flow Solutions and Prevention of Voltage Collapse in System with Induction Motor Load

朴 鍾 根*
(Jong-Keun Park)

요 약

잘 알려진 바와 같이 電力潮流方程式은 最多 2^{N-1} 개의 電壓解를 가질 수 있다. 이 論文에서는 모드(mode)槪念을 導入하여 이 電壓解를 特性지웠다. 즉(+) 및 (-) 모드 전압으로 定義하였다. (-)모드의 전압은 電力用 콘덴서에 대해서(+) 모드의 電壓과 거의 반대로 應動한다.

또한 유동전동기부하를 갖는 계통의 전압붕괴 현상의 방지에 대하여 考察하였다. 電力用콘덴서의 連續制御 및 不連續制御로서 電壓을 制御할 경우에 各 制御器가 가져야할 特性의 臨界値를 計算하고 유도전동기부하와 임피던스부하의 구성비가 이臨界値에 미치는 영향에 대해서 檢討하였다.

Abstract

As is well known, the power equations of the N-node system have 2^{N-1} voltage solutions at most. The voltage solutions are characterized by the introduction of the mode concept in this paper. There are two mode voltages at one node. One is defined as the (+) mode voltage and the other is defined as the (-) mode one. In this paper, we show that the (-) mode voltage responds to the increase of the power condenser almost adversly to the response of the (+) one.

We study how to prevent the voltage collapse in the system with the induction motor load. The critical values of the gain and the time constant in case of the continuous power condenser control, and of the unit power condenser and the closing time delay in case of the discontinuous control for the prevention of the voltage collapse, are calculated. The effect of the composition ratio of the impedance load to the induction moter load on the above critical values are also investigated.

1. Introduction

Stability analysis has been performed for the planning and the operation of power system. Conventional stability analysis has been concenturated on the power stability analysis, and power angles among generators are considered to be the most important factor to influence the stability of power system.

In recent years, however, much attention has been paid to the voltage collapse phenomenon at the load side due to the current tendencies such that,

a) generators do not have sufficient capability to supply reactive power to the load any more on account of the immense reactive power loss of long and bulky transmission lines, and
b) the capacity of constant power consuming load such as air conditioner is increasing year by year.

*正 會 員 : 서울대 工大 電氣工學科 助敎授 · 工博
接受日字 : 1984年 10月 31日

The voltage collapse phenomena have been experienced in France[8] and Soviet Union, as well as in Japan. Therefore, the analysis of voltage collapse phenomenon has become a new important topic. The voltage phenomenon has very close relations with the voltage characteristics of the load and with the performance of reactive power supplying equipment. It is also very closly related with the multisolution problem of the power flow (to be explained in section 2.1).[1],[2],[3]

This paper deals with

a) the difference of characteristics between the (+) mode and the (−) mode voltage solutions. Supposing the voltages of all nodes except one node are fixed, there exist two values of the voltage at one node. We define one as the (+) mode voltage and the other as the (−) mode voltage. Before the resonance point is reached the value of the former solution increases with the increase of the power condenser admittance, but the value of the latter decreases. After the resonance point is exceeded the reverse tendency appears, except that the latter do not begin to rise until the admittance of power condenser is increased beyond a certain value.

b) the prevention of the voltage collapse in the system with the I.M. (induction motor) load. Although power system does not ordinarily operate in the (−) mode region, large disturbances may bring the system into the (−) mode operating condition.

We show that the voltage collapse can be prevented by the discontinuous control of the power condenser well as by the continuous control of the power condenser or LRT (load ratio transformer). The critical values of the gain and time constant in case of the continuous control, and of the unit power condenser and closing time delay in case of the discontinuous control are calculated for the prevention of the voltage collapse. The effect of the composition ratio of impedance load to induction motor load on the above critical values is investigated.

2. The difference of characteristics between (+) mode and (−) mode voltage

2.1 Introduction of mode concept

Power equations of the N-node system have 2^{N-1} voltage solutions at most, as is well known, when load flow calculations are performed for power system analysis. In this section the mode concept of the voltage solution is introduced.

The schematic diagram in Fig. 1 shows the N-node system used for the introdution of the mode concept. The power equation of the system at node i is as follows:

$$P_i + jQ_i = \dot{V}_i \sum_{k \in si} \{(\frac{\dot{V}_k}{\dot{Z}_{ki}}) - (\frac{\dot{V}_i}{\dot{Z}_{ki}})\}^* + j Y_{ci} V_i^2 \tag{1}$$

where P_i and Q_i are the active and reactive powers flowing from from node i respectively, $\dot{Z}_{ki}$ is the impedance between nodes k and i, $\dot{V}_i$ is the voltage of node i, and S_i is the set of the nodes interconnected directly to node i. The term $\sum_{k \in si} \dot{V}_k/\dot{Z}_{ki}$ in eq. (1) stands for the short circuit current when node i is shorted and it can be expressed as

$$\dot{I}_i \triangleq \sum_{k \in si} \dot{V}_k/\dot{Z}_{ki} = I_{i1} + j I_{i2} = I_i \varepsilon^{j\phi i} \tag{2}$$

where $$I_{i1} \triangleq \sum_{k \in si} \frac{R_{ki} \cos \delta_k + X_{ki} \sin \delta_k}{R^2_{ki} + X^2_{ki}} V_k ,$$

$$I_{i2} \triangleq \sum_{k \in si} \frac{R_{ki} \sin \delta_k - X_{ki} \cos \delta_k}{R^2_{ki} + X^2_{i}} V_k$$

From eqs. (1) and (2), we obtain eq. (3)

$$P_i + G_i V_i^2 + j (Q_i + B'_i V_i^2) = \dot{V}_i \dot{I}_i^* \tag{3}$$

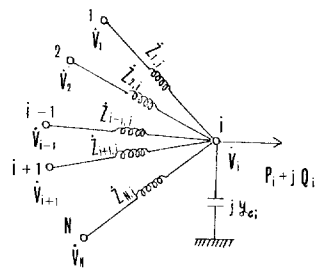

Fig. 1. Network of N-node system.

where G_i is $\sum_{k \in si} R_{ki} / (R^2_{ki} + X^2_{ki})$, the equivalent conductance seen from node i, B_i is $\sum_{k \in si} X_{ki} / (R^2_{ki} + X^2_{ki}) - Y_{ci}$, the equivalent susceptance.

There are four variables V_i, δ_i, P_i, Q_i at each node of the power system. In the load flow calculation two variables are given and the other two should be calculated. When P and Q are given at a node, the node is called P-Q node. When P and V are given at a node, the node is called P-V node. Supposing the voltages of all nodes except node i are fixed, there exist two values of the voltage magnitude at P-Q node i with regard to given active power P_{is} as shown in Fig. 2. In Fig. 2, we define the voltage corresponding to point A as the (+) mode voltage, and that corresponding to point B as the (−) mode voltage. From eq. (3) V_i is obtained as follows:

$$V_i = \left[\frac{-(2P_i G_i + 2Q_i B'_i - I_i^2) \pm \{(2P_i G_i + 2Q_i B'_i) * 2(G_i^2 + B'^2_i) * - I_i^2)^2 - 4(G_i^2 + B'^2_i)(P_i^2 + Q_i^2)\}^{1/2}}{2(G_i^2 + B'^2_i)} \right]^{1/2} \quad (4)$$

In eq. (4), because I_i is the function of $V_1, \ldots, V_{i-1}, V_{i+1}, \delta_1, \ldots, \delta_{i-1}, \delta_{i+1}, \ldots, \delta_N$, eq. (4) can be reexpressed as follows:

$$V_{i+} = f_{i+}(P_i, Q_i, V_1, \ldots, V_{i-1}, V_{i+1}, \ldots, V_N, \delta_1, \ldots, \delta_{i-1}, \delta_{i+1}, \ldots, \delta_N)$$

$$V_{i-} = f_{i-}(P_i, Q_i, V_1, \ldots, V_{i-1}, V_{i+1}, \ldots, V_N, \delta_1, \ldots, \delta_{i-1}, \delta_{i+1}, \ldots, \delta_N) \quad (5)$$

where f_{i+} stands for the function of (+) sign in the complex sign of eq. (4) and f_{i-} stands for that of (−) sign. Furthermore angle δ_i is given as follows:

$$\delta_i = \tan^{-1}\left\{\frac{I_{i1}(Q_i + B'_i V_i^2) + I_{i2}(P_i + G_i V_i^2)}{I_{i1}(P_i + G_i V_i^2) - I_{i2}(Q_i + B'_i V_i^2)}\right\}$$

$$= g_i(P_i, Q_i, V_1, \ldots, V_N, \delta_1, \ldots, \delta_{i-1}, \delta_{i+1}, \ldots, \delta_N) \quad (6)$$

substituting V_{i+} for V_i when node i is in the (+) mode condition and V_{i-} when node i is in the (−) mode condition, we have

$$\delta_{i+} = g_i(P_i, Q_i, V_1, \ldots, V_{i-1}, V_{i+}, V_{i+1}, \ldots, V_N, \delta_1, \ldots, \delta_{i-1}, \delta_{i+1}, \ldots, \delta_N)$$

$$\delta_{i-} = g_i(P_i, Q_i, V_1, \ldots, V_{i-1}, V_{i-}, V_{i+1}, \ldots, V_N, \delta_1, \ldots, \delta_{i-1}, \delta_{i+1}, \ldots, \delta_N) \quad (7)$$

In the same way, there also exist two values of the reactive power at P-V node i with regard to given active power P_{is} as shown in Fig. 3. In Fig. 3, we define the angle corresponding to point A as the (+) mode angle and that corresponding to point B as the (−) mode angle.

Performing the load flow calculation of the model system shown in Fig. 4 on the basis of the above mode concept, we have the result as shown in Figs. 5(a) & (b). The changes of the solutions with regard to the

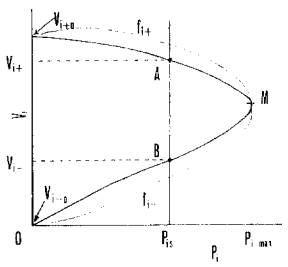

Fig. 2. P-V curve.

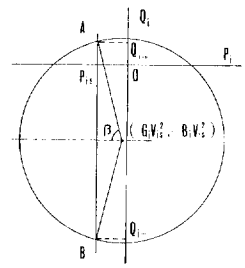

Fig. 3. Relation between P and Q.

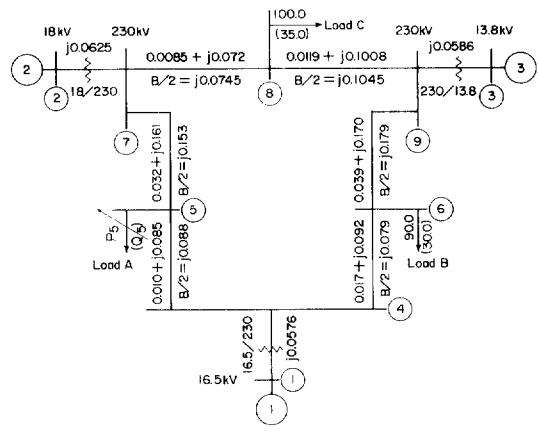

All impedances are in pu on a 100-MVA base

Fig. 4. 9-bus model system.

changes of load C are shown in Fig. 5(a). In the figure, curves a, b and c represent the voltages of node 5,6 and 8 respectively. the parts of the curves drawn in the sign x respresent the solutions when node 5 in the (−) mode condition with other nodes (+) modes, and the parts of curves drawn in the sign · represent the solutions when node 5 is in the (+) mode condition. It is important here to mention that the increase of the power condenser admittance at the (−) mode node causes the decrease in the voltage of the (−) mode node as shown in Fig. 5(b) in case node 5 is (−) mode. It is reverse to the case of (+) mode. In Fig. 5(b) SC_5 is the power condenser inserted at node 5.

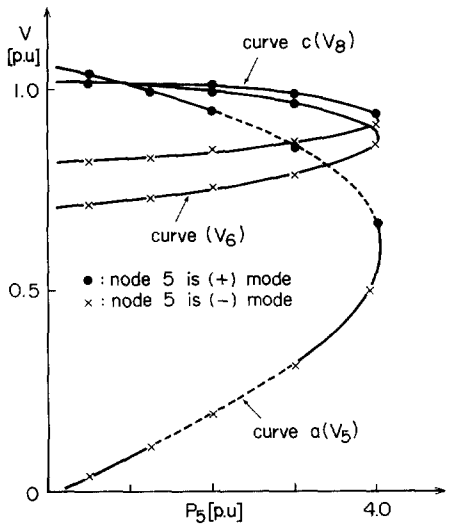

Fig. 5(a). Voltages of load nodes when node 5 is (−) mode.

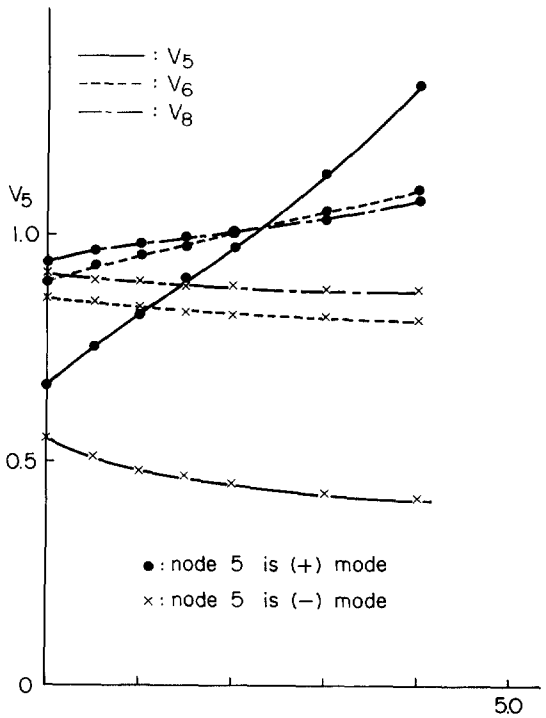

Fig. 5(b). Changes of V_5 with increase of SC_5.

2.2 The difference of characteristics between (+) mode and (−) mode voltages

The circuit diagram shown in Fig. 6 shows the equivalent circuit for the power system network in Fig. 1, when seen from node i. It is postulated in Fig. 6 that resistances of the transmission lines are zero, and that the load is represented by the variable admittance which gives the constant power consuming load independently of the variation of the voltage From the power equilibrium equation at node i, we have

$$f(y_i) = X_i^2 S_i y_i^2 + \{ 2 X_i S_i (1 - X_i y_{ci}) \sqrt{1-\cos^2\varphi_i} - E_i^2 \}$$
$$y_i + S_i (1 - X_i y_{ci})^2 \qquad (8)$$

where $\cos\varphi_i$ is the power factor of load, X_i is the equivalent inductance of transmission lines, S_i is the magnitude of load, $y_i = \sqrt{g_i^2 + b_i^2}$, and y_{ci} is the admittance of the power condenser inserted at node i.

The function $f(y_i)$ with various y_{ci}'s is plotted in Fig. 7. Eq. (8) has two solutions of y_i, which give two values of voltage V_i as follows:

$$V_i = \sqrt{S_i} / \sqrt{y_i} \qquad (9)$$

In Fig. 7 the solutions in the area I are equivalent to the (+) mode voltages explained in the previous section, and the solutions in the area II are equivalent to the (−) mode voltages.

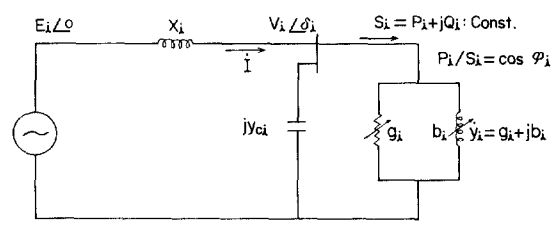

Fig. 6. Equivalent circuit

When $y_{ci} < 1/X_i$ (Fig. 7(a)), the solution y_i in the area I becomes smaller as y_{ci} becomes larger, which means that the more power condenser has to be inserted for the higher voltage. Adversly, the solution y_i in the area I becomes smaller as y_{ci} becomes larger, which means that the more power condenser has to be inserted for the higher voltage. Adversly, the solution y_i in the area II becomes larger as the power condenser admittance y_{ci} becomes larger, which means that the more power condenser is inserted, the lower the voltage becomes.

When $y_{ci} = 1/X_i$, $f(y_i)$ has the solution zero in the area I, which means that there is a resonance point in the (+) mode region.

When $y_{ci} > 1/X_i$ (Fig. 7(b)), the reverse tendency is observed in Area I. However, in area II the same tendency is observed as that when $y_{ci} < 1/X_i$ by a certain value of y_{ci} which is determined by the power factor and the magnitude of load. But over that y_{ci} there happens the reverse tendency to that when $y_{ci} < 1/X_i$. The change of voltage $\dot{V}_i$ corresponding to the change of power condenser admittance y_{ci} is plotted with various magnitudes of load in Fig. 8(a) and (b).

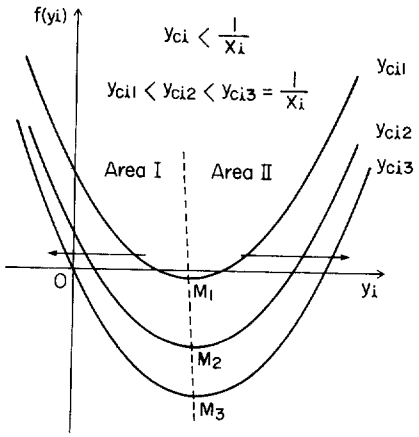

Fig. 7(a). $f(y_i)$ when $y_{ci} \leqq 1/X_i$.

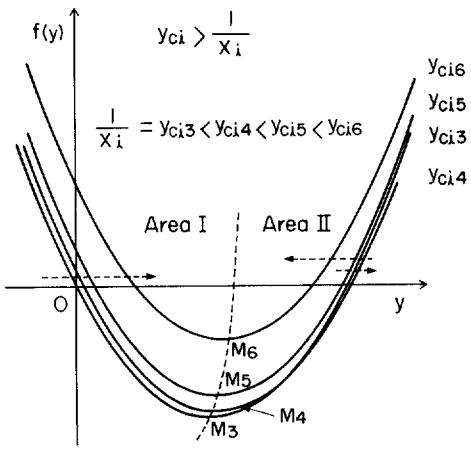

Fig. 7(b). $f(y_i)$ when $y_{ci} \geqq 1/X_i$.

3. Prevention of voltage collapse in systems with induction motor load

The behavior of voltage $\dot{V}_r$ of the I.M. load node corresponding to large disturbances is shown in Fig. 9. The system does not ordinarily operate on the part of B-M in curve 1, which is the (−) mode region. But large disturbances such as large voltage drop near power sources, the opening of transmission line and the dropping of generator, bring the system into operating in the (−) mode region. In this region the voltage of the I.M. load node is unstable and collapses at any disturbance. Therefore, some control is necessary to prevent the voltage from collapsing when the system is brought into operating in the (−) mode region for

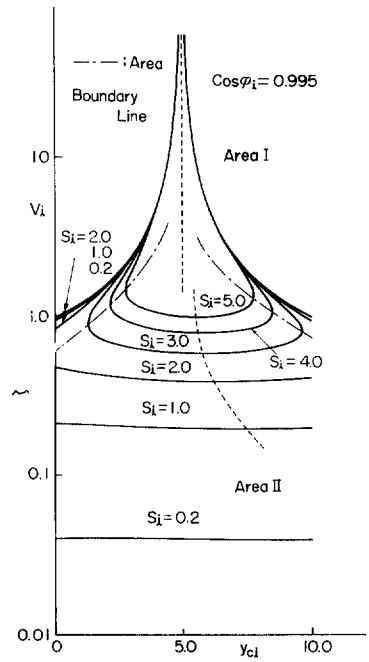

Fig. 8(a). V_i y_{ci} curves with various S_i's when $\cos\varphi_i = 0.995$

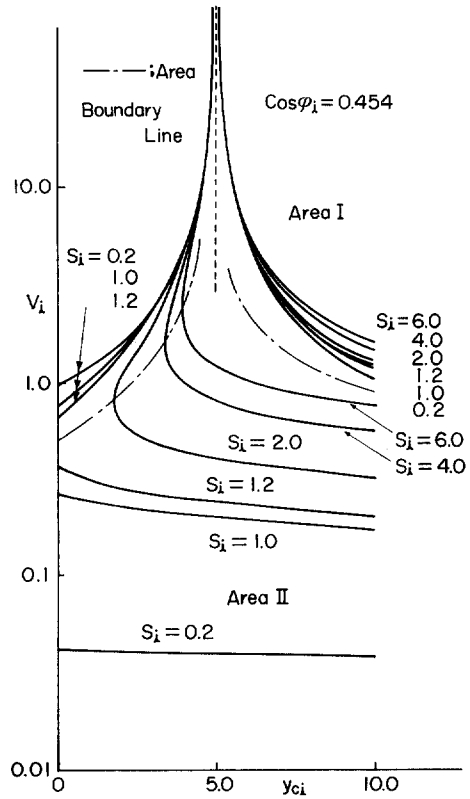

Fig. 8(b). V_i-y_{ci} curves with various S_i's when $\cos\varphi_i = 0.454$

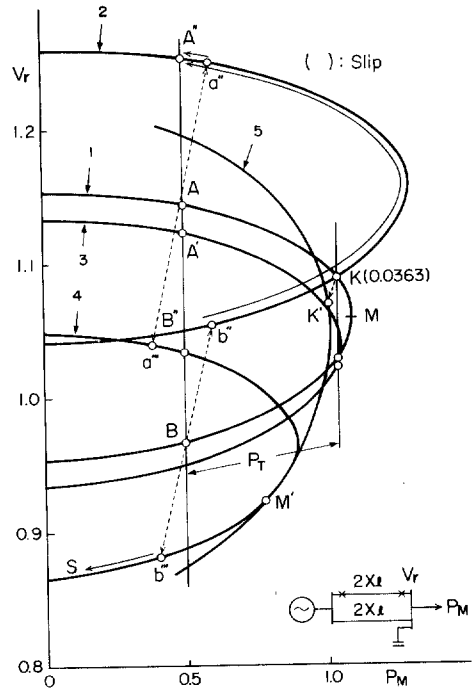

Fig. 9. Transient behavior of V_r.

some causes. In this section the prevention of the voltage collapse in the system with I.M. load, which is a typical nonlinear load, is investigated.

3.1 The transient behavior of the voltage of the I.M. load node

The schematic diagram in Fig. 10 shows the details of the model system that has been used for numerical simulation.[6],[7]

In the transient state, the motion of I.M. can be described by the following equation;

$$-H\frac{ds}{dt} = P_M - P_T,$$

$$P_M = \frac{m^2 r_o b_l^2 V_s^2 s}{s^2 (1 - m^2 X_m Y)^2 + m^2 r_o^2 Y}$$

$$b_l = -1/x_l,\ Y = y_c + b_l \qquad (10)$$

where P_M is the eletrical input power to I.M., m is the

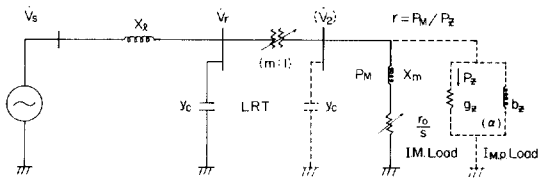

Fig. 10. Model system with I. M. load.

turn ratio of LRT, and P_T, s, H are axial load, slip, inertia of I.M. In Fig. 9, curves 1, 2, 3, and 4 show the static characteristic curves for V_s = 1.1, 1.2, 1.08 and 1.0.(p.u) with X_l fixed at O.1.(p.u) If V_s increases stepwise while the system operates at point A with the (+) mode voltage, the operating point moves to point a" corresponding to the same slip as the slip of point A, and settles down stably at point A" which is the equilibrium point of the electrical input power and the axial load. On the other hand, if V_s drops stepwise, the operating point moves in the sequence A → a" → A". In case that V_s rises stepwise from operation point B of the (−) mode voltage, the operating point does not settle down in the sequence B → b" → B", but settles down at point A", the (+) mode voltage, in the sequence B → b" → A". If V_s drops, induction motor stops and the voltage

collapses after the operating point moves in the sequence B → b″ → S. Curve 5 shows the static characteristic curve for x_t = 0.2 (p.u) which is twice of the reactance in curve 1, with V_s fixed at 1.1. If one circuit of transmission line is cut off due to a fault while the system operates at point K, the operating point moves to point K′. Here, unless the system recovers the former state, double circuit system, by the time the operating point reaches point M′, the operating point moves into the (−) mode region at last, because the load is larger than the maximum capacity of transmission power of one circuit tranamission line.

3.2 Prevention of voltage collapse

Linearizing eq. (10) around a certain operating point, we have

$$-H\frac{d\Delta s}{dt}=\frac{\partial P_M}{\partial s}\Delta s+\frac{\partial P_M}{\partial y_c}\Delta y_c+\frac{\partial P_M}{\partial m}\Delta m-\Delta P_T \tag{11}$$

Eq. (11) has a poitive eigen value in the (−) mode region and the system is unstable in that region.
Fig. 11 shows the behavior of the voltage and the slip when the system is unstable.

As the power condenser is conventionally switched on or off to control its output power, each variable varies as shown in Fig. 12(b). Fig. 12(a) shows the control block diagram. The kicks in Fig. 12(b) show the

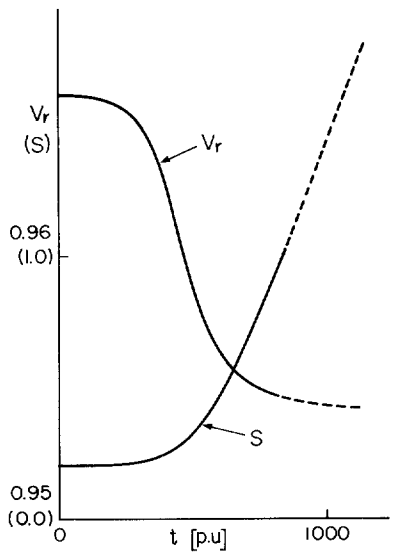

Fig. 11. Behaviors of V_r & s when system unstable.

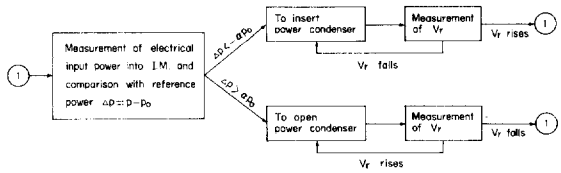

Fig. 12(a). Control block diagram.

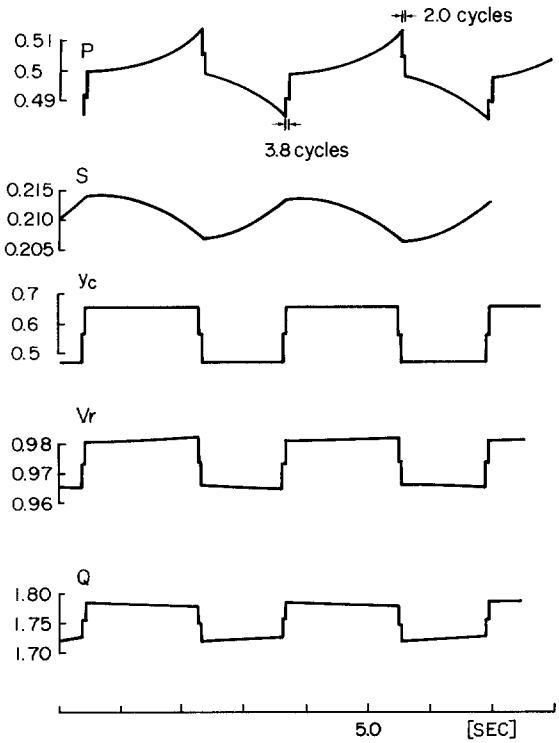

Fig. 12(b). Behavior of each variable on discontinuous control.

time delay for control error measurement and power condenser switching. Each variable varies periodically under the above control. However, supposing the power condenser could be continuously controlled as indicated in eq. (12), each variable varies as shown in Fig. 14(a), (b) and (c).

$$\Delta y_c=\frac{K_c}{1+T_c p}\Delta s \tag{12}$$

$$\Delta m=\frac{K_m}{1+T_m p}\Delta s \tag{13}$$

where Δs is the variation of induction motor slip s Eq. (13) is the transfer function of the LRT control.

We have the block diagram expressed in terms of the varible s from eqs. (11) and (12) shown in Fig. 13(a), where m is 1.0 which means, the control of LRT is not performed simultaneously. Deriving s expressed in terms of V_r and y_c from the power equilibrium at the load node, we have

$$s = r_o (Y^2 V_r^2 - b_l^2 V_s^2)^{1/2} \{b_l^2 x_m^2 V_s^2 - (Y x_m - 1)^2 V_r^2\}^{1/2} = f_1(V_r, y_c) \quad (14)$$

From eqs. (10) and (14), we have

$$\frac{dV_r}{dt} = h_1(V_r, y_c) + h_2(V_r, y_c, P_T) + h_3(V_r, y_c) \quad (15)$$

where

$$h_1 = \frac{(b_l^2 V_s^2 - Y^2 V_r^2)\{(Yx_m - 1)^2 V_r^2 - x_m^2 b_l^2 V_s^2\}^2}{H r_o V_r (1 - 2 Y x_m)^2 b_l^2 V_s^2}$$

$$h_2 = -\frac{(b_l^2 V_s^2 - Y^2 V_r^2)^{1/2}\{(Yx_m - 1)^2 V_r^2 - b_l^2 V_s^2}{H r_o V_r (1 - 2 Y x_m) b_l^2 V_s^2} \frac{x_m^2\}^{3/2}}{} P_T$$

$$h_3 = -\frac{V_r (Y V_r^2 - x_m Y^2 V_r^2 - x_m b_l^2 V_s^2)}{(1 - 2 Y x_m) b_l^2 V_s^2} \frac{dy_c}{dt}$$

We have the block diagram expressed in terms of the variable V_r from eqs. (12), (14) and (15) as shown in Fig. 13(b).

The numerical simulations that have been carried out in the model system shown in Fig. 10 with the power mismatch between the electrical power input and the shaft load as the disturbance show the behavior of

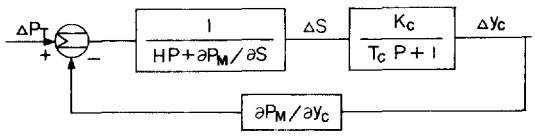

Fig. 13(a). Block diagram expressed in s.

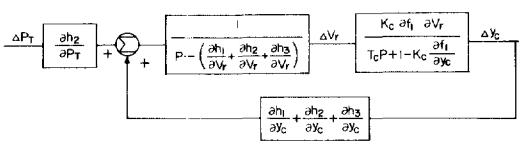

Fig. 13(b). Block diagram expressed in V_r

y_c and s as shown in Fig. 14(a). The larger the gain K_c is, the less the quantity of the finally necessary power condenser output power to prevent the voltage from collapsing is. Fig. 14(b) shows the behavior of y_c and s with various time constants. As the time constant of controller gets closer to the per unit value of the inertia of induction motor, each variable oscillates. Fig. 14(c) shows the behavior of V_r and s behave as shown in Figs. 14(a) & (b).

In order that the voltage V_r is prevented from collapsing in the (−) mode region, there are critical values of the unit of y_c in case of the discontinuous control, and of K_c and T_c in case of the continuous control. Fig. 15 shows the relations between the critical value of the unit and the closing time delay of the power condenser. The opening time delay does not usually matter in case of the power condenser control, because the closing time delay is longer than the opening one. Here, how to read Fig. 15 is explained by an example. If the iner-

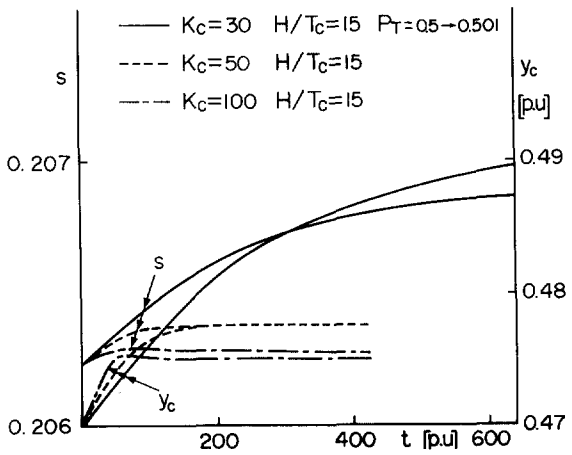

Fig. 14(a). Behavior of each variable with various K_c

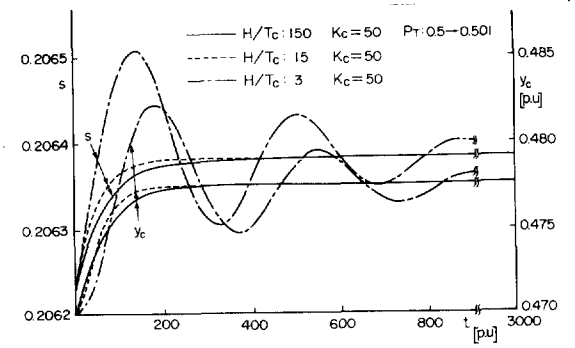

Fig. 14(b). Behavior of each variable with various T_c's.

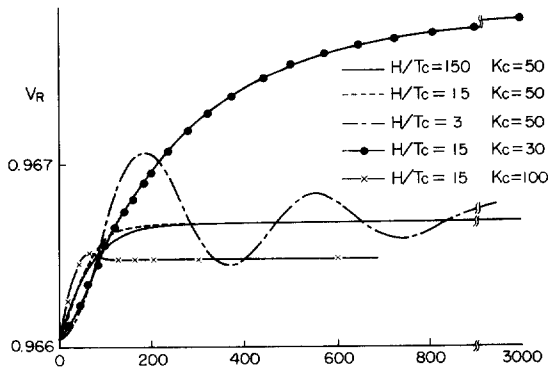

Fig. 14(c). Behavior of V_r.

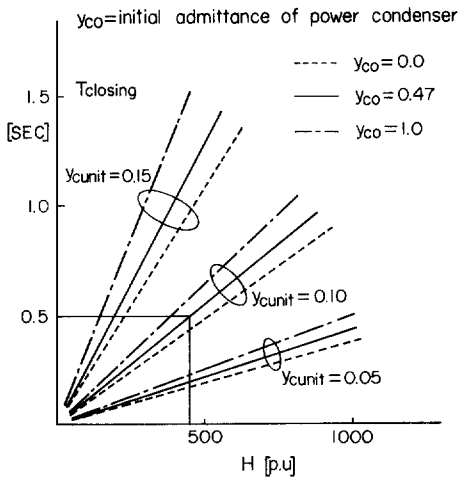

Fig. 15. Relation among critical values on discontinuous control.

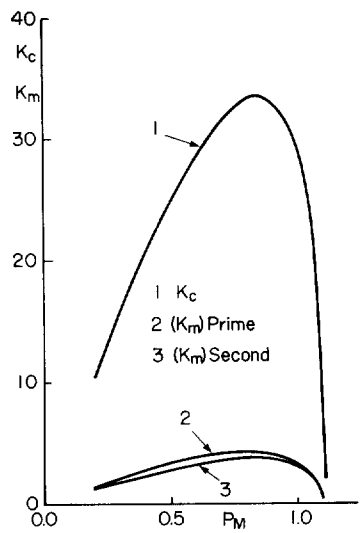

Fig. 16. Critical K_c's in I.M. load.

tia of I.M., the closing time delay and the initial value of the power condenser admittance are 450(p.u), 0.5(sec) and 0.47(p.u), the critical control unit of y_c is 0.1(p.u). In other words, $T_{closing}$ should be shorter than 0.5(sec) when the control unit of y_c, y_{co} and H are 0.1(p.u), 0.47(p.u) and 450(p.u), or the control unit of y_c should be larger than 0.1(p.u) when y_{co}, H and $T_{closing}$ are 0.47(p.u), 450(p.u) and 0.5(sec), in order that the voltage be prevented from collapsing.

Fig. 16 shows the critical gain when the power condenser or LRT is controlled continuously as shown in eq. (12) or eq. (13). Curve 1 shows the critical value of K_c. Curve 2 shows the critical value of Km when the power condenser is inserted on the primary side of LRT, and curve 3 shows that of LRT when the power condenser is inserted on the secondary side. In Fig. 16, V_r is prevented from the collapse on the region above curve 1, 2 or 3. The area above curve 3 is wider than that above curve 2. Consequently it is more effective to insert the power condenser on the secondary side than to insert it on the primary side from the viewpoint of the voltage collapse prevention.

How the composition ratio of the impedance load to the I.M. load affects on the critical gain is shown in Fig. 17 where α (or b_z/g_z) is the factor with corresponds to the power factor of the impedance load, and γ (or Pz/Pm) is the radio of the impedance load to the I.M. load. The prevention of the voltage collapse is able to be accomplished by adopting gain constant Kc determined by Fig. 17. This means the system is

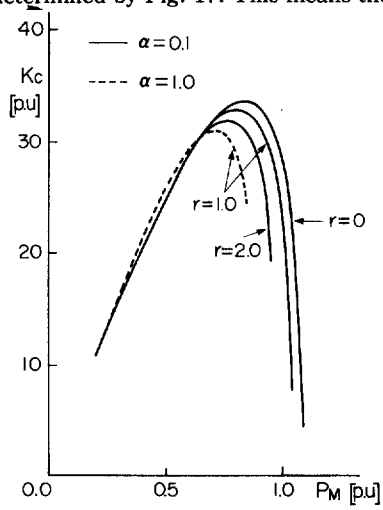

Fig. 17. Critical K_c's in composite load.

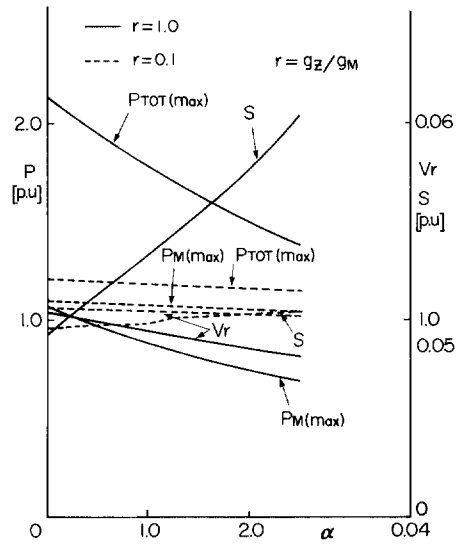

Fig. 18. Maximum transmissable power.

stable when the gain is greater than the critical gain. It can be observed from Fig. 17 that it is easier to keep the system stable when the ratio of the impedance load to the I.M. load is bigger. It can be also seen that the worse power factor of the impedance load makes it easier to keep the system stable.

However, the worse power factor makes the maximum capacity of transmission power less as shown in Fig. 18. In the figure, P_M (max) is the maximum transmitted power to I.M. and P_{TOT} (max) is the total maximum transmitted power to I.M. and the impedance load. V, and s are the values of the voltage and the slip when the transmitted power is at maximum.

4. Conclusion

We have shown in this paper that the static voltage response of power system operating at the (−) mode voltage to the increase of the power condenser admittance is almost reverse to that at the (+) mode voltage. The (+) mode voltage causes a resonance when the admittance of inserted power condenser is equal to $1/X_l$, where X_l is the equivalent inductance of the transmission lines.

The voltage collapse in the system with the I.M. load is able to be prevented by the control of the power condenser or LRT. There exist the critical values of the gain and the time constant in case of the continuous control, and of the power condenser admittance unit and the closing time delay in case of the discontinuous control. In case of the LRT control, it is more effective for the prevention of the voltage collapse to insert the power condenser on the secondary side of LRT than to insert it on the primary side. The more impedance load is in parallel with the I.M. load, the easier it is to keep the system stable.

Acknowledgements

The author would like to express his sincere appreciation to professor Y. Sekine, Tokyo Univ. for his good advices.

The author also would like to express his sincere appreciation to Korea Science And Engineering Foundation for its financial support.

References

1) J. Park & Y. Sekine: "A Method for Analyzing Multisolution in Power Flow Analysis (in Japanese).", Trans. IEE of Japan, 99-B, 245 (Apr. 1979)
2) A. Yokoyama & Y. Sekine: "Multisolutions for Load Flow Problem of Power System and Their Physical Stability Test (in Japanese).", Trans. IEE of Japan, 100-B, 509 (Sep. 1980)
3) A. Klos & A. Kerner: "The Nonuniqueness of Load Flow Solution", 5th PSCC Cambridge (1975)
4) G. Shackshaft & P.H. Ashmole: "The Influence of Load Characteristics on Power System Performance", CIGRE 31-02 (1978)
5) T. Nagao: "Voltage Stability Analysis (in Japanese)", J. IEE of Japan, 100, 16 (Jan. 1980)
6) K. Goto & Y. Sekine: "Research on Voltage Collapse (in Japanese)", Denryokukenkyukai, IEE of Japan, ET-75-7 (May 1975)
7) J. Park & Y. Sekine: "Prevention of Voltage Collapse in System with I.M. load (in Japanese)." Conference, IEE of Japan, No. 859 (1981)
8) C. Barbier & J. P. Barret: "An Analysis of Phenomena of Voltage Collapse on a Transmission System.", RGE-Special Issue, 3 (July 1980)